

# Accurate, fast and generalisable first principles simulation of aqueous lithium chloride.

Junji Zhang<sup>1</sup>, Joshua Pagotto<sup>1</sup>, Tim Gould<sup>2</sup>,  
Timothy T. Duignan<sup>1,2\*</sup>

<sup>1</sup>School of Chemical Engineering, University of Queensland,  
Brisbane, QLD 4072, Australia.

<sup>2\*</sup>Queensland Micro- and Nanotechnology Centre, Nathan, Qld 4111,  
Australia, Griffith University, Nathan, QLD 4111, Australia.

\*Corresponding author(s). E-mail(s): [t.duignan@griffith.edu.au](mailto:t.duignan@griffith.edu.au);

## Abstract

Electrolyte solutions play a pivotal role throughout chemistry and biology. For over a century, scientists have therefore sought to accumulate a precise knowledge and understanding of their thermodynamic, kinetic, and structural properties. However, the vast majority of electrolyte properties have not *or cannot* be determined empirically, despite being key to understanding a huge range of biological and chemical processes and systems. In this work, we introduce a long-sought-after solution to this problem and employ it to develop a detailed understanding of an electrolyte solution: aqueous lithium chloride. Our solution draws from recent breakthroughs in machine learning, first principles quantum chemistry and statistical mechanics and lets us develop and run truly predictive all-atom and coarse-grained simulations using long-range corrected equivariant neural network potentials (NNP). Surprisingly, our calculations reveal the formation of Li cation dimers. This previously unknown species highlights the power of the approach to divulge new understanding of electrolytes. Key electrolyte properties, including activity and diffusion coefficients, are determined from first principles and validated in close agreement with experiment. The training data is a small set (655 frames) of moderate-cost density corrected density functional theory (DC-DFT) calculations, meaning the approach can be scaled to build a database of electrolyte solution properties.

**Keywords:** Solutions, liquids, ion-ion interactions, ion diffusivities, thermodynamic properties, kinetic and structural properties, ab initio molecular dynamics, equivariant neural network potentials, coarse grained models.

## Introduction

Liquids are the most important phase of matter. Essentially all of biology occurs in the liquid phase, as does much of chemical engineering and climate science. They are also notoriously difficult to model or simulate due to their disordered dynamic nature combined with their sensitivity to complex quantum mechanical interactions. Recent breakthroughs in machine learning and quantum chemistry are enabling a paradigm shift towards the prediction of the properties of liquids starting from first principles.[1–4]

Electrolyte solutions are a particularly important class of liquids, that are even more challenging to model due to the inclusion of long range electrostatic interactions. The prediction of their properties from first principles is a foundational problem of physical chemistry that has remained unsolved despite over a century of effort.

Electrolytes are ubiquitous and play an active and central role in a vast range of important processes and systems. For example, lithium cations are the primary charge carrier for Li-ion batteries and their chemical equilibria and diffusivities impact the assembly and performance of these devices.[5, 6] Remarkably, lithium also exhibits important biochemical effects such as its efficacy as a treatment for bipolar disorder. However, electrolytes are important in such a wide range of systems that highlighting individual cases does not properly convey the scope of applications.

The ability to accurately and efficiently predict the properties of electrolyte solutions from first principles would be transformative. Firstly, it would provide direct insight into the molecular scale details that determine key macroscopic properties. These insights could be used to guide the design and optimisation of electrolytes for the many important applications where they play a key role. Secondly, it could be used to generate large data sets of molecular scale information.[7] Such a database would be invaluable for training machine learning models that are capable of generalising to an even wider range of situations,[8] analogous to the way the protein data bank was leveraged to train AlphaFold2.[9]

The foundational model of electrolytes (Debye-Hückel theory) was developed a century ago this year. It is based on continuum solvent theory and gives a quantitative description of the thermodynamic and structural properties of electrolytes but only at millimolar concentrations.[10, 11] At any practically relevant concentrations, the theory must be corrected using empirically adjusted parameters. The Pitzer model is the most common example of this approach and it forms the basis for the calculation of thermodynamic properties of electrolytes in modern chemical engineering.[12, 13]

This reliance on empirical data to predict the properties of electrolyte solutions is a critical problem. It means that for any case where good empirical data does not exist, time consuming experimental characterisation combined with trial and error is required to understand and optimise electrolyte solution behaviour. While excellent experimental databases have been built for some electrolyte solution properties,[13, 14] they are inherently limited to a relatively small number of cases.[15]

First Principles Molecular Dynamics (FPMD) based on ab initio or density functional theory[16–19] is the only approach that avoids this dependence on empirical data. However, the extremely large computational demands of this technique limit its

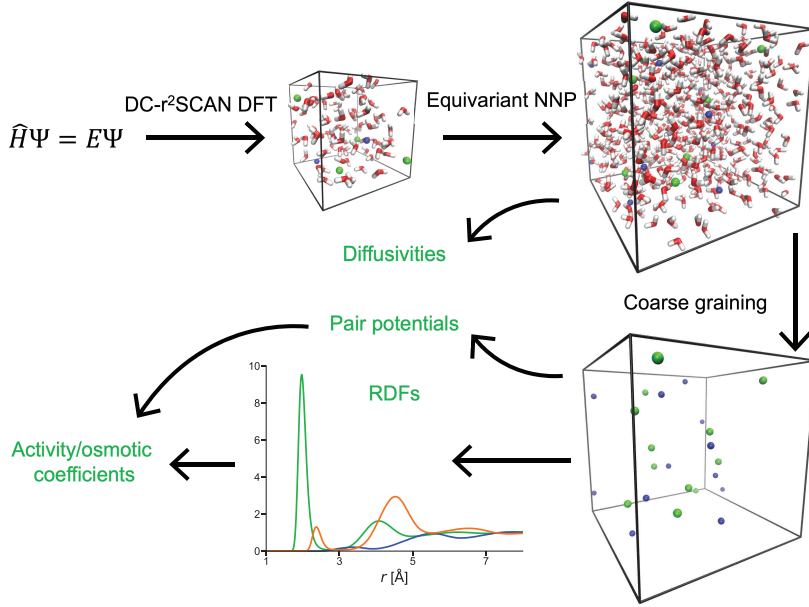


**Fig. 1: Simulation overview** Small, short FPMD simulations are run with CP2K. Energies/forces are recomputed with the DC-r<sup>2</sup>SCAN DFA. This data set is then used to train an equivariant NNP which enables much larger simulations with a larger cell. Forces and coordinates of the ions alone are output from the NNP-MD and used to train a coarse grained NNP, which enables much faster MD simulations and the calculation of key structural, thermodynamic and kinetic properties.

direct applicability to small systems and a few properties. Additionally, many current density functional approximations (DFAs) have inaccuracies. [20–23]

Two exciting new tools enable the transformation of FPMD into a dramatically more useful tool. The first is density corrected DFT (DC-DFT) which significantly reduces the errors (delocalisation and self interaction) that lead standard density functional approximations (DFAs) to inaccurately describe ions. This method generally uses a Hartree-Fock electron density as input into the strongly constrained and appropriately normalised (SCAN) DFA. It has shown particularly promising results recently, including for aqueous ionic systems. [24–29]

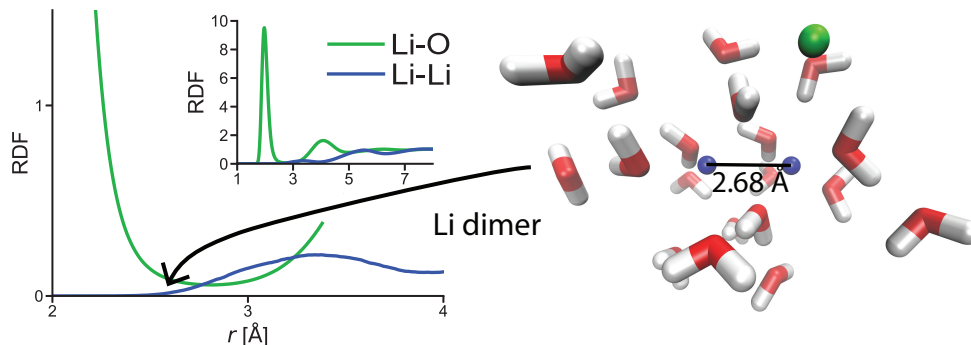


**Fig. 2: Lithium dimer formation** Lithium oxygen, and lithium lithium RDFs demonstrate the formation of lithium cation dimers that penetrate into the first hydration layer and an example snapshot from the MD simulation, showing the water molecules and nearest chloride ion surrounding the dimer.

The second tool is a new generation of Neural Network Potentials (NNP)[30–37] that incorporates equivariance[38–42] and explicit electrostatics.[32, 43–46] This approach trains a neural network to reproduce the mapping between coordinates and energies/forces to massively accelerate FPMD simulation.[30–37] Equivariance means that the rotational symmetries of 3D Euclidean space are encoded into the neural network. These improvements enable significantly more accurate, reliable and generalisable NNPs. It has also been demonstrated that NNPs enable coarse grain molecular dynamics simulation enabling further acceleration.[47–50] More generally machine learning potentials are an incredibly exciting new tool for helping understand many systems, including electrolytes.[2, 5, 43, 45, 46, 51–53, 53–65]

Here, we perform equivariant all atom and coarse grained NNP-MD simulations of aqueous lithium chloride with explicit long-range electrostatics described by a continuum solvent model. Density corrected regularised SCAN (DC-r<sup>2</sup>SCAN) is used to generate the training data. We observe the remarkable formation of Li cation dimers and demonstrate excellent agreement with experimental structural, kinetic, and thermodynamic properties. Figure 1 provides an overview of the workflow used in this study.

## Results and Discussion

### Lithium dimer formation

The most surprising revelation from the simulations was the formation of lithium cation dimers, shown in Figure 2, where one lithium penetrates into the first solvation layer around another lithium ion. The first solvation layer is defined by the first minima in the Li-O RDF which is 2.8 Å. The smallest separation of the lithium ions observed in the simulations (2.68 Å) matches the separation of the neutral covalent dilithium. (2.67 Å) and is much smaller than the Li-Li distance in LiCl crystal of 3.62 Å. The formation of this species is particularly surprising given that this ions an archetypal

kosmotrope or water structuring ion. Physically this was believed to correspond to the formation of a tightly bonded first solvation layer of water molecules that was thought to be impenetrable to other ions.[66]

Ironically, the cation dimer appears to be stabilised by lithium’s kosmotropic behaviour, i.e., the strong structuring of water around the lithium leaves a region of minimal water density in between the first two hydration layers that the co-ion can occupy.

This remarkable and counter-intuitive finding may have important implications for the many biological and chemical systems where lithium plays a critical role.[6] The transient nature of this pair means that this species could not feasibly be identified with direct FPMD simulation. CMD simulations show no indication of it,[67] which is likely attributable to the neglect of charge transfer and polarisation effects which will significantly mitigate the electrostatic repulsion. Given the surprising nature of this finding it is crucial to carefully validate the reliability and robustness of these simulations as we do in the following sections.

## Low training data requirements

The training data for the NNP, trained with NequIP,[39] consists of a strikingly small training data set of only 655 frames extracted from MD simulation computed at the DC-r<sup>2</sup>SCAN level of theory with CP2K.[18, 29, 68] The 655 frames each contain 4 Li<sup>+</sup> and 4 Cl<sup>-</sup> ions along with 80 water molecules. The faster r<sup>2</sup>SCAN level of theory was used to generate the initial trajectory, which was then re-sampled with DC-r<sup>2</sup>SCAN.

The total computational cost of generating this dataset was very reasonable, i.e., on the order of tens of thousands of CPU hours. It is therefore feasible to scale this approach to many different electrolyte solutions and build a large database of properties. By contrast, non-equivariant NNP architectures generally require much larger training data sets or demand active learning algorithms to build the data set. Additional details on how the training data generation are outlined in the Computational Methods section below.

## Long, large and accurate simulations

Two NNPs were trained (NNP1 and NNP2) on the DC-r<sup>2</sup>SCAN data set using different random seeds for the weight initialisation and for splitting the data into training and validation sets. NNP-MD was performed with NNP1 on the original sized cell and 200 frames were extracted from the simulation and recomputed with DC-r<sup>2</sup>SCAN level of theory. Figure 3a demonstrates that the NNP is very accurately estimating the forces with an RMSE below 10 meVÅ<sup>-1</sup>.

Parallel simulations were then run for 2.4 ns each with both NNP1 and NNP2 on a system six times bigger than the original ( 25.26<sup>3</sup> Å<sup>3</sup> vs. 13.87<sup>3</sup> Å<sup>3</sup>) containing 512 water molecules and 48 ions. Accessing this time and spatial scale is entirely infeasible with direct FPMD critical, yet is critical for studying ion-ion correlations which have long range structure that is larger than the cell size used for FPMD. The NNP-MD generates 200 ps per day for the larger system on a single V100 GPU.

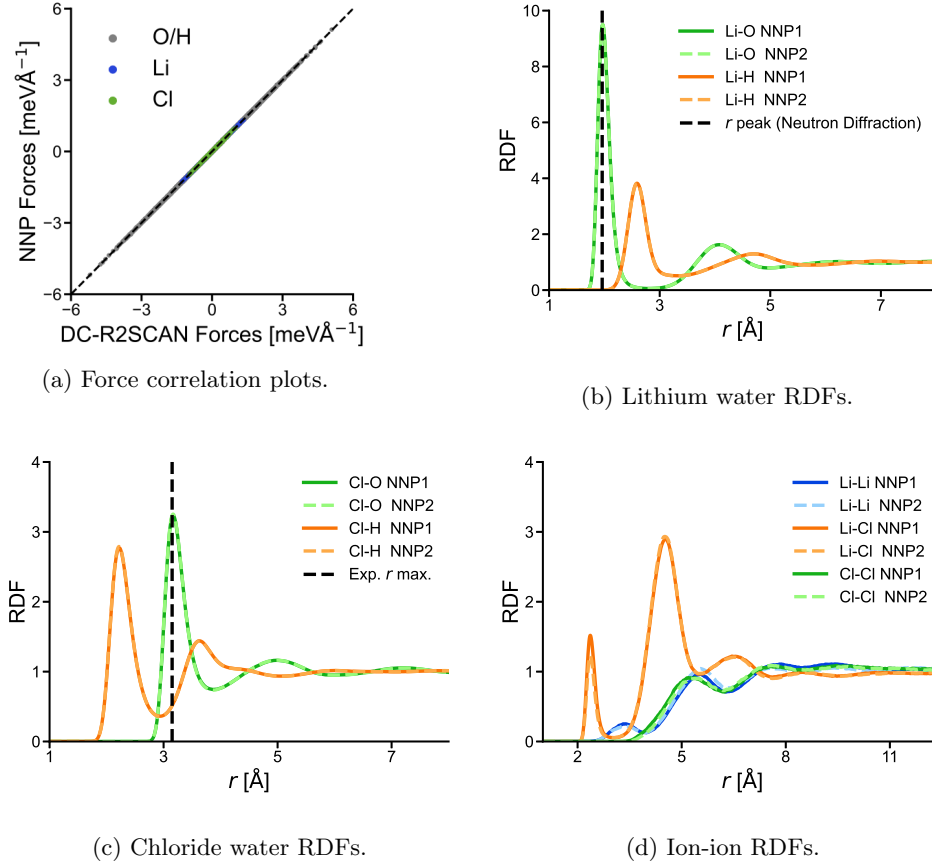


**Fig. 3: Consistency checks of the NNP.** (a) Comparison of the forces computed at the DC-DFT level of theory with the predictions of the NNP for 200 frames extracted from a NNP-MD simulation. (b),(c) and (d) compare the RDFs predictions of two NNPs trained with different initial seeds demonstrating consistency. Good agreement with neutron diffraction measurements of the peak in the ion oxygen RDF is also observed.

Figure 3b,3c and 3d compares the ion-solvent and ion-ion radial distribution functions (RDFs) computed with the two separate NNPs showing excellent agreement and demonstrating convergence and the reproducibility of the method. The ion-oxygen peak positions of 1.97 and 3.17 Å are in good agreement with neutron diffraction measurements of 1.96 and 3.15 Å for lithium and chloride respectively.[69] The first shell coordination number at 4.2 and 6.9 with the NNP-MD are also very consistent with experimental values of 4.1 and 7 from neutron diffraction.[69]

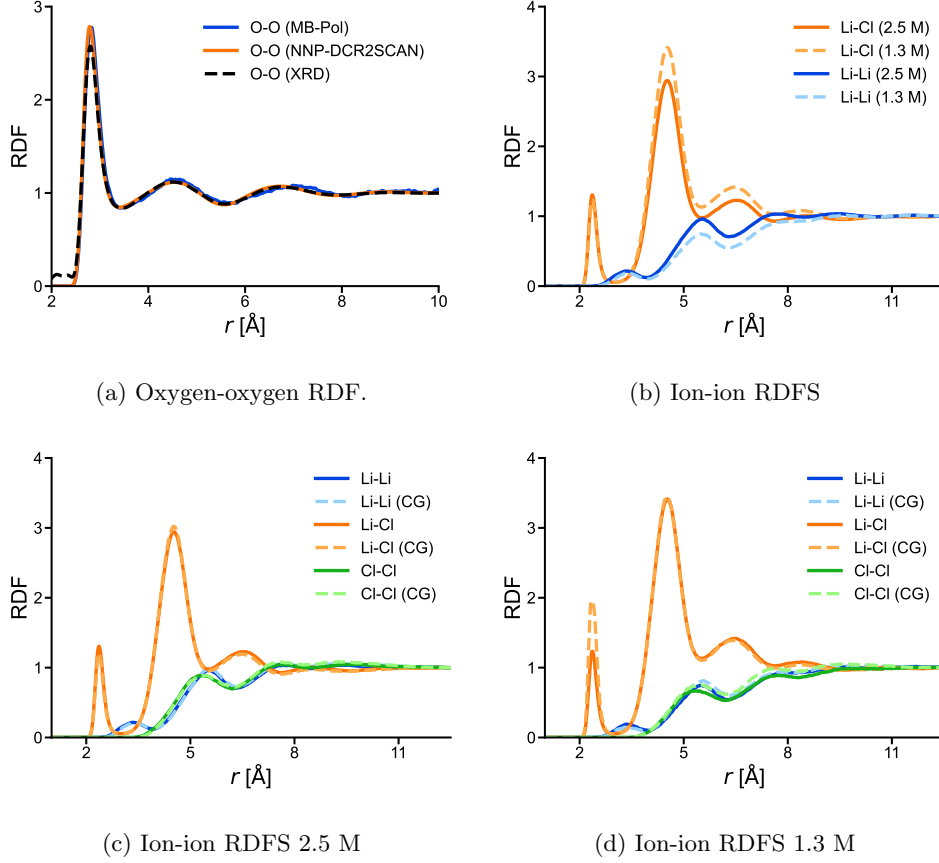


**Fig. 4:** (a) Comparison of the predicted O-O RDF with a pure water NNP-MD simulation with experimental X-Ray Diffraction measurements[70] and the MB-pol water model.[71] (b) Comparison of ion-ion RDFs at the concentration of 2.5 M with a lower concentration (1.3 M) which the model was not trained on. (c,d) Comparison of the all atom and coarse grained ion-ion RDFs predicted at 2.5 M (c) and 1.3 M (d) showing good agreement.

## Generalisability to lower concentrations

It is important to validate the NNPs description of the water-water interactions. The structural properties of water, such as the oxygen-oxygen RDF, computed at 2.5 M are difficult to verify experimentally. However, to test the NNPs description of the pure water interactions we can run a pure water simulation. Remarkably Figure 4a shows essentially perfect agreement with experimental X-ray diffraction measurements. The small difference in the first peak height is attributable to the neglect of quantum nuclear effects, which is verified by comparison with MB-Pol, a state of the art water model.

The fact that without any explicit effort to fit to or reproduce the properties of pure water we arrive at a model that gives such accurate structural predictions is particularly promising and demonstrates the generalisability of this approach.

To further test the generalisability of the method simulations were performed at 1.3 M using the same NNPs. Similarly stable simulations were observed with no physical inaccuracies. Most promisingly an increasing Debye-Hückel screening length is visible in these simulations as the concentration decreases. The fact that NNP-MD can reproduce this effect despite using training data from a single concentration is promising.

## Coarse Graining

The all atom NNP-MD is much faster than FPMD and capable of simulating experimentally relevant timescales but the computational cost is still non-trivial and more expensive than most CMD approaches. To remedy this we build a coarse grained model of the electrolyte solutions, more specifically we integrate out the solvent degrees of freedom resulting in a continuum or implicit solvent model. To do this we use the NNP to learn the potential of mean force, which is a free energy surface. The problem of learning a free energy surface is very similar to learning the full all-atom potential energy surface and so also benefits from equivariance as has recently been demonstrated.<sup>[48]</sup> As before we compute the long range electrostatic interactions separately using the known analytical expression.

In practice to do this we extract the coordinates and forces for the ions alone for 24,000 frames extracted from a 2.4 ns NNP-MD all atom simulation. A larger data set is required to sufficiently converge the averaging over the solvent degrees of freedom. It would not be feasible to generate such a large training data set with FPMD directly but is straightforward with NNP-MD. The coarse grain NNP requires many fewer weights and trains very quickly in comparison to the all atom NNP due to the much simpler energy surface.

The coarse grained MD can reproduce the RDFs from the all atom MD accurately as shown in Figure 4c. It is also reasonably generalisable as shown in Figure 4d where it reproduces the RDF at 1.3 M including the decrease in long range screening. This is impressive considering that we only trained on data from a single concentration.

The coarse grained NNP-MD is orders of magnitude faster than the all atom NNP and requires trivial computational resources to fully converge, i.e, tens of CPU hours. This hierarchical layering of NNPs where a coarse grained NNP is trained on a lower level data from all atom NNP demonstrates a promising general approach to the long standing challenge of connecting scales in molecular simulation. <sup>[72, 73]</sup>

## Empirical validation

While there is no way to directly validate the ion-ion RDFs, as they cannot be accurately determined experimentally, their reliability can be indirectly validated by comparison with thermodynamic properties. Specifically, the activity coefficients as a function of concentration have been shown to be highly sensitive to the strength of the



ion-ion interactions. The accurate prediction of these quantities gave the original validation of Debye-Hückel theory. The ability to determine these properties accurately is also of immense practical importance for chemical engineering.

Here, we use Kirkwood-Buff theory to compute the derivative of the activities at 2.5 and 1.3 M, with good experimental agreement as shown in Figure 5a for both the all atom MD and coarse grained MD RDFs. The coarse grained predictions have negligible error bars due to their better convergence. The all atom MD is used for the ion-water RDFs, which converge much more quickly than the ion-ion RDFs and make a very small contribution to the total.

Diffusivities of  $\text{Li}^+$  and  $\text{Cl}^-$  ions as well as water molecules are also in good agreement with experiment as shown in Figure 5b. This is particularly impressive as kinetic properties depend on accurately assessing barrier heights in the potential energy surface. These will be poorly represented in the training data set as it is extracted from equilibrium molecular dynamics.

A direct relative of the activity coefficients, the osmotic coefficients, can also be approximately computed using a modification of Debye-Hückel’s theory. The key requirement is the infinite dilution potential of mean force (PMF), also known as the pair potential. This is a fundamental quantity that can be inserted into the Poisson-Boltzmann equation and solved to compute electrostatic potential and RDFs at any concentration with trivial computational cost. A virial expression can then be used to convert these to osmotic coefficients.

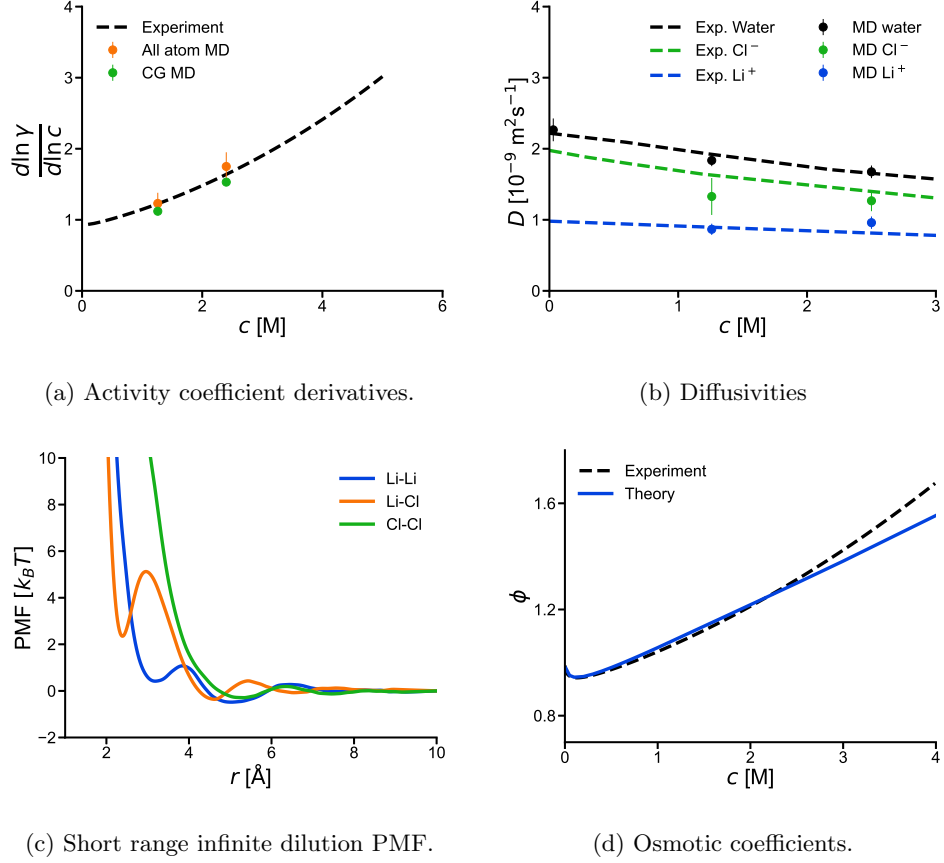
Computing the infinite dilution PMF is normally an extremely challenging task requiring enhanced sampling techniques, such as umbrella sampling with very low concentration simulations. Here we can trivially extract this quantity from the coarse grained NNP by simply computing the interaction energy between the three ion pairs in isolation. These infinite dilution PMFs are shown in Figure 5c with the long range Coulomb term removed. A correction term is included to account for the variation in the dielectric constant as a function of concentration between the training concentration of 2.5 M and infinite dilution.

Figure 5d shows the theoretically predicted osmotic coefficients demonstrating good agreement with experiment. These can be directly converted to activity coefficients using the Gibbs-Duhem relation. The experimental values are converted from Lewis-Randall to Macmillan-Mayer scheme as required.[75, 76]

## Conclusion and future work.

In summary, we have demonstrated the accurate prediction of the structural, kinetic and thermodynamic properties of aqueous LiCl electrolyte solution. Our approach combines the exciting new tools of equivariant NNPs and DC-DFT with the century old mathematical theory of electrolytes. Despite its remarkable predictive ability, it has very low training data requirements and requires relatively few computational resources.

The prediction of these properties, particularly activity coefficients, has been a key goal of physical chemistry for over a century. This is firstly because they play a critical role in huge range of important applications and secondly because the reproduction



**Fig. 5:** (a) Comparison of activity coefficient derivatives predicted with Kirkwood-Buff theory using both all atom and coarse grained MD at two concentrations. (b) Comparison of the computed diffusivities with experimental values[74] for water and both ions at two concentrations and infinite dilution also showing good experimental agreement. (c) The infinite dilution potential of mean force between the two ions computed with the coarse grained NNP. (d) Comparison of osmotic coefficients computed with the short ranged infinite dilution PMF and the modified Poisson-Boltzmann equation.

of these properties is an important validation of the reliability and accuracy of these methods, which is a necessary prerequisite to the accurate simulation of many more complex systems.

The next step is to begin scaling this method to build a database of properties of electrolytes across a much wider range of conditions and compositions than exists currently. A key focus should be on important electrolytes that are particularly difficult to characterise experimentally such as pure lithium bicarbonate which immediately

speciates into a mixture of carbonates in solution, meaning even its most basic properties have never been measured. More advanced techniques for generating the data sets such as meta-dynamics[77] and active learning[61, 65] will likely be required for these more complex systems.

Besides being of direct practical use, this database can also provide the training data for a new generation of AI models analogous to Alphafold2’s use of the PDB.[9] This should enable the rapid prediction of the properties of electrolyte solutions, without requiring direct simulation. Such a database could also be used to train generative models for designing new electrolytes.[78]

## Computational Methods

### FPMD (CP2K)

We used Born-Oppenheimer *ab initio* molecular dynamics simulations within a constant volume NVT (300 K) ensemble with periodic boundary conditions. The CP2K simulation suite (<http://www.cp2k.org>) containing the *QuickStep* module for the DFT calculations [18, 68] was used with a 0.5 fs time step. We used a double  $\zeta$  basis set that has been optimized for the condensed phase[79] in conjunction with GTH pseudopotentials [80] optimised for SCAN[81, 82] and a 1200 Ry cutoff.[83, 84] A Nosé-Hoover thermostat was attached to every degree of freedom to ensure equilibration. [85]

An  $\approx 10$  ps simulation was run consisting of 4 lithium ions, 4 chloride ions and 80 water molecules in a cell of fixed dimensions of  $13.87^3 \text{ \AA}^3$ , corresponding to an electrolyte concentration of 2.5 M. The cell size was adjusted to match the experimental density at this concentration. The initial simulation used the r<sup>2</sup>SCAN DFA.[24]

458 frames were extracted from this initial simulation in addition to 197 frames from a 1 ns NNP-MD simulation trained on it. (see below for details) The forces were then recomputed on these 655 frames using the density corrected r<sup>2</sup>SCAN DFA. [26, 27] This method has recently been implemented in CP2K[29]. The auxiliary density matrix method (ADMM) was employed to improve the scaling of the four-center two-electron integrals.[86] The Schwarz integral screening threshold was set to  $10^{-5}$  units. A contracted auxiliary basis set (cFIT3) was used to construct the auxiliary density matrix.

### NNP fitting (NequIP)

The training data set was generated as follows: 1) 458 (70%) frames were sampled directly from a 10 ps FPMD run using r<sup>2</sup>SCAN; 2) a trial NNP was fit to the r<sup>2</sup>SCAN forces, and used to generate 1 ns of NNP-MD data with the FPMD box size; 3) the remaining 197 (30%) frames were then sampled from the 1 ns NNP-MD run, to improve the diversity of training data for the more sophisticated NNP resulting in total of 655 frames.

The trial r<sup>2</sup>SCAN was fit to 985 frames. The 655 frames of DC-r<sup>2</sup>SCAN calculations from both the FPMD and the NNP-MD were used to train two new neural networks, referred to as NNP1 and NNP2 above.

As our NNP only has access to local information, (short range,  $< 5 \text{ \AA}$ )[44] the long range electrostatic ion-ion interactions were removed from the forces and energies prior to training. These were computed using a dielectrically screened Coulomb interaction.[87] They were then added back in during all NNP-MD simulations.

The same hyperparameters were used for all of the all atom NNPs. More specifically 100:1 weighting on forces vs energies was used in the default loss function.[39] We decrease the initial learning rate of 0.01 by a decay factor of 0.5 whenever the validation RMSE in the forces has not seen an improvement for five epochs. Training was stopped when the learning rate is smaller than  $10^{-5}$ . The model with the lowest validation error was used for simulations. A radial cutoff distance of  $5 \text{ \AA}$  was used. Three layers of interaction blocks were used with the maximum  $l$  set to 2 each with 16 features. Only even parity was used. Invariant neurons for the radial network was set to 32. All the other parameters were set to the defaults. A 80:20 training validation split was used throughout.

For all the NNPs the Coulomb interactions screened by the dielectric constant of water (78.3) between all the ions were subtracted before training. These were calculated with LAMMPS by placing appropriately screened charges on the ions to reproduce dielectric screening of 78.3 and with the particle-particle particle-mesh method.[88]

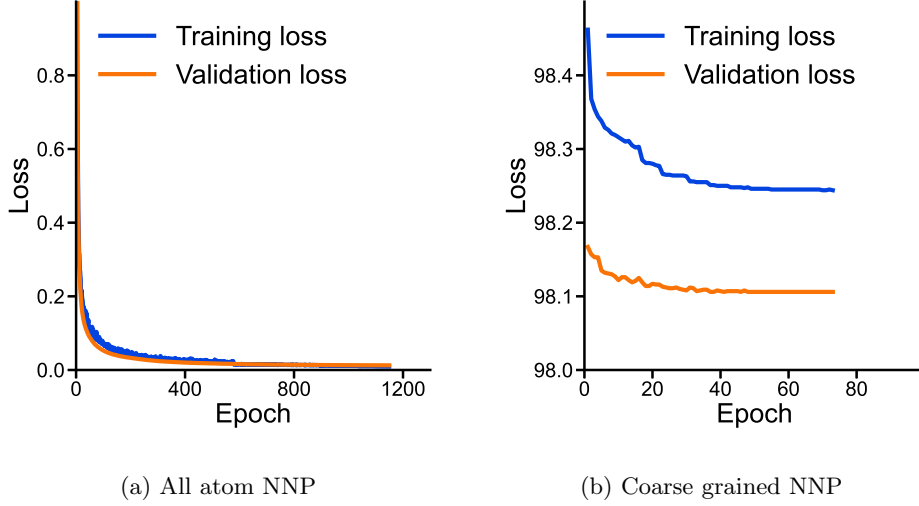
To train the NNP for the coarse grain MD we found that reducing the number of parameters was important to provide stability. Two layers of interaction blocks were used with the maximum  $l$  set to one each with 8 features. Only even parity was used. Invariant neurons for the radial network was set to 8. All the other parameters were set to the defaults. The radial cut off was also extended to  $10 \text{ \AA}$  to provide longer range interactions.

Figure. 6a and 6b show the learning curves. RMSE on the validation set for the first all atom NNP (NNP1) was  $8.9 \text{ meV/\AA}$  for the forces and  $0.11 \text{ meV}$  for the energies. For NNP2 it was  $9.7 \text{ meV/\AA}$  for the forces and  $0.12 \text{ meV}$  for the energies. The RMSE on the ions is much higher with the coarse grained model as expected due to the neglect of the solvent. They were  $299 \text{ meV/\AA}$  for the forces and  $38 \text{ meV}$  for the energies. Remarkably the error on initialisation was  $302 \text{ meV/\AA}$  and  $91 \text{ meV}$  respectively meaning that training of the NNP only removed  $3 \text{ meV/\AA}$  in error and yet this is enough to reliably reproduce the ion-ion RDFs.

## NNP MD (NequIP/LAMMPS)

The NequIP plugin for LAMMPS[89] was used to perform several NVT simulations at 300 K for 2.4 ns. A Nosé-Hoover thermostat was attached to every degree of freedom to ensure equilibration [85]. The long-range Coulomb interactions were added to the simulation using LAMMPS hybrid overlay method. No initial data was discarded as the initial frame was taken from the end of the AIMD simulation.

We use constant volume simulations with the experimental density to estimate the cell size to avoid relying on experimental information. The 2.5 M simulations in the larger cell size had dimensions of  $25.26^3 \text{ \AA}^3$  and contained 48 ions and 512 water molecules. The 1.3 M simulations had a  $25.05^3 \text{ \AA}^3$  cell size with 24 ions and 512 water molecules. Three 2.4 ns simulations were run at 2.5 M and four at 1.2 M to



**Fig. 6:** Learning curves

ensure convergence. Most simulations were very stable with no noticeable non-physical behaviour except for one simulation at 2.5 M where water molecule deprotonated with the hydrogen forming a tight bond with lithium. This trajectory was not used.

VMD[90] was used to create the RDFs and images in Fig. 1.

The infinite dilution PMFs were computed in LAMMPS by simply computing the total energy of the system of two ions in a  $25.26^3 \text{ \AA}^3$  as a function of distance. At short distances, where the NNP has no data as the ions do not approach closely, the NNP can oscillate randomly. At these points an increasing extrapolation was used to ensure that the infinite dilution PMF didn't go negative again.

### Modified Poisson-Boltzmann Equation (MPBE)

The dielectric Coulomb potential was removed analytically to determine the short range contribution to the infinite dilution PMF and a correction was included in the short range potential, i.e., between 2 and 10  $\text{\AA}$  to account for the change in dielectric constant between 2.5 M and infinite dilution. The correction is given by:

$$\frac{qe}{4\pi\epsilon_w r} - \frac{qe}{4\pi\epsilon_s r} \quad (1)$$

where the dielectric constant of bulk water was given by:  $\epsilon_w = 78.3$  and the dielectric constant of the solution at 2.5 M is given by  $\epsilon_s = \frac{78.3}{1+\beta\rho}$ . This is a standard expression used to compute the concentration dependence of the dielectric constant.[91] We use the value of  $\beta = 0.19$ .

The infinite dilution PMF was then used in the MBPE to compute the electrostatic potential and RDFs at 17 concentrations between 0.01 and 4 M. The MPBE is given

by:

$$-\epsilon_r \epsilon_o \frac{1}{r^2} \frac{d}{dr} \left( r^2 \frac{d\phi(r)}{dr} \right) = \sum_i q_i \rho_i(r) \quad (2)$$

Where the density is given by:

$$\rho_i(r) = \rho_i \exp[-\beta (q_i \phi(r) + W_{\text{SR}}(r))] \quad (3)$$

$\frac{\rho_i(r)}{\rho_i}$  corresponds to the RDF. The boundary conditions used to solve the MPBE are the electric field of a point charge at 2 Å and the electric potential of 0 at large separations (60 Å). These settings ensure reliable numerical solutions are found using the shooting method implemented in Mathematica.[92] Smoothing was applied to the PMFs to improve the convergence of the numerical differential equation solution.

Note that there are two ways to solve the MPBE one with the cation as the central ion and one with the anion. The choice does not materially effect the predicted osmotic coefficients though.

### Osmotic coefficients calculation

The MPBE can determine RDFs down to infinite dilution with minimal computational demands.  $W_{\text{SR}}(r)$  can then be input into the virial expression for the osmotic coefficients to estimate them at many concentrations.[67, 93, 94]

$$\phi(\rho) = 1 - \frac{\pi}{3} \rho \sum_{i,j} \int_0^\infty g_{ij}(r) \frac{dW_{ij}(r)}{dr} r^3 dr \quad (4)$$

where  $W_{ij}(r)$  is the ion-ion infinite dilution PMF, i.e.,  $W_{\text{SR}}(r)$  plus the Coulomb interaction, i.e., the full infinite dilution PMF. This gives reasonable agreement with osmotic coefficients as shown in the main text.

Experimental densities[95–97] were used to convert theoretical osmotic coefficients from the McMillan-Mayer to the Lewis-Randal level to enable the correct thermodynamic comparison.[75, 76] Experimental values are obtained from the Pitzer equations and converted to molarity again using experimental densities.[98] A fixed dielectric constant was used in the MPBE as this corresponds best with underlying McMillan-Mayer level the theory is based on, i.e., fixed solvent chemical potential.

The Gibbs-Duhem relationship between osmotic and activity coefficients could be used to convert osmotic coefficients into activities if desired.

### Kirkwood-Buff theory calculations.

Kirkwood-Buff theory [99] was used to compute the derivatives of the activities from the RDFs with the following expressions:

$$\frac{1}{1 + \rho (G_{\text{cc}} - G_{\text{co}})} \quad (5)$$

where  $\rho$  is the ion density.  $G_{cc}$  is given for a monovalent ions by:

$$G_{cc} = \frac{1}{4} (G_{++} + G_{--} + 2G_{+-}) \quad (6)$$

and  $G_{co}$  is given by:

$$G_{co} = \frac{1}{2} ((G_{+O} + G_{-O})) \quad (7)$$

where the  $G$  refers to the Kirkwood-Buff integrals:

$$G_{ij} = \int_0^\infty (g_{ij}(r) - 1) r^2 dr \quad (8)$$

The integrals were cutoff at half the box size and the RDFs were normalised by their average value around 1 Å of the cutoff to ensure they went to 1. For the coarse grained MD results the ion-solvent integrals were computed using the coarse-grained MD.

## Diffusion coefficients calculation

Diffusion coefficients were computed from the mean squared displacements (MSD) of the water molecule and lithium and chloride ions in our NNP MD trajectories. This conversion was carried out using the diffusion coefficient-MSD relationship described below:

$$D = \frac{\text{MSD}}{6t} \quad (9)$$

The results were finally adjusted by finite size corrections [100]. Here, we have used the experimental value (0.888 mPas) for the viscosity of pure water when determining the finite size correction. Experimental values were obtained from Ref. 74.

## Acknowledgements

We acknowledge Stefan Vuckovic, Debra Bernhardt, Christopher Mundy, Gregory Schenter, Simon Batzner, Alby Musaelian, Sophie Baker, Alister Page, Juerg Hutter and Andrey Bliznyuk for helpful discussions and computational assistance. TTD was supported by an Australian Research Council (ARC) Discovery Project (DP200102573) and DECRA Fellowship (DE200100794). TG was supported by an Australian Research Council (ARC) Discovery Project (DP200100033) and Future Fellowship (FT210100663). This research was undertaken with the assistance of resources and services from the National Computational Infrastructure (NCI), which is supported by the Australian Government and with the assistance of resources from QCIF. (<http://www.qcif.edu.au>)

## References

- [1] Deringer, V. L. *et al.* Origins of structural and electronic transitions in disordered silicon. *Nat* **589**, 59–64 (2021).

- [2] Galib, M. & Limmer, D. T. Reactive uptake of N<sub>2</sub>O<sub>5</sub> by atmospheric aerosol is dominated by interfacial processes. *Science (New York, N.Y.)* **371**, 921–925 (2021).
- [3] Kapil, V. *et al.* The first-principles phase diagram of monolayer nanoconfined water. *Nat* **609**, 512–516 (2022).
- [4] Bore, S. L. & Paesani, F. Realistic phase diagram of water from “first principles” data-driven quantum simulations. *Nat. Commun.* **14**, 3349 (2023).
- [5] Hellström, M. & Behler, J. Structure of aqueous NaOH solutions: Insights from neural-network-based molecular dynamics simulations. *Phys. Chem. Chem. Phys.* **19**, 82–96 (2017).
- [6] Chen, X. & Zhang, Q. Atomic Insights into the Fundamental Interactions in Lithium Battery Electrolytes. *Accounts Chem. Res.* **53**, 1992–2002 (2020).
- [7] Gregory, K. P., Elliott, G. R., Wanless, E. J., Webber, G. B. & Page, A. J. A quantum chemical molecular dynamics repository of solvated ions. *Sci. Data* **9**, 430 (2022).
- [8] Winter, B., Winter, C., Esper, T., Schilling, J. & Bardow, A. SPT-NRTL: A physics-guided machine learning model to predict thermodynamically consistent activity coefficients. *Fluid Phase Equilibr.* **568**, 113731 (2023).
- [9] Jumper, J. *et al.* Highly accurate protein structure prediction with AlphaFold. *Nat* **596**, 583–589 (2021).
- [10] Debye, P. & Hückel, E. Zur Theorie der Elektrolyte. I. Gefrierpunktserniedrigung und Verwandte Erscheinungen [The Theory of Electrolytes. I. Lowering of Freezing Point and Related Phenomena]. *Phys. Z.* **24**, 185–206 (1923).
- [11] Robinson, R. A. & Stokes, R. H. *Electrolyte Solutions* (Butterworth & Co., Devon, 1959).
- [12] Pitzer, K. S. Thermodynamics of electrolytes. I. Theoretical basis and general equations. *J. Phys. Chem.* **77**, 268–277 (1973).
- [13] May, P. M. & Rowland, D. Thermodynamic Modeling of Aqueous Electrolyte Systems: Current Status. *J. Chem. Eng. Data* **62**, 2481–2495 (2017).
- [14] Rowland, D. & May, P. M. Progress in Aqueous Solution Modelling: Better Data and Better Interfaces. *J. Solution Chem.* **48**, 1066–1078 (2019).
- [15] Vaque Aura, S. *et al.* Data Analysis for Electrolyte Systems: A Method Illustrated on Alkali Halides in Water. *J. Chem. Eng. Data* **66**, 2976–2990 (2021).



- [16] Marx, D. & Hutter, J. *Ab Initio Molecular Dynamics: Basic Theory and Advanced Methods* (Cambridge University Press, Cambridge, 2009).
- [17] Baer, M. D. & Mundy, C. J. Toward an Understanding of the Specific Ion Effect Using Density Functional Theory. *J. Phys. Chem. Lett.* **2**, 1088–1093 (2011).
- [18] Kühne, T. D. *et al.* CP2K: An Electronic Structure and Molecular Dynamics Software Package I. Quickstep: Efficient and Accurate Electronic Structure Calculations. *J. Chem. Phys.* **152**, 1–51 (2020).
- [19] Duignan, T. T., Kathmann, S. M., Schenter, G. K. & Mundy, C. J. Toward a First-Principles Framework for Predicting Collective Properties of Electrolytes. *Accounts Chem. Res.* **54**, 2833–2843 (2021).
- [20] Riera, M., Mardirossian, N., Bajaj, P., Götz, A. W. & Paesani, F. Toward chemical accuracy in the description of ion–water interactions through many-body representations. Alkali-water dimer potential energy surfaces. *J. Chem. Phys.* **147**, 161715 (2017).
- [21] Paesani, F., Bajaj, P. & Riera, M. Chemical accuracy in modeling halide ion hydration from many-body representations. *Advances in Physics: X* **4**, 1631212 (2019).
- [22] Wagle, K. *et al.* Self-Interaction Correction in Water – Ion Clusters. *J. Chem. Phys.* **154**, 094302 (2021).
- [23] Duignan, T. T., Schenter, G., Mundy, C. J. & Zhao, X. S. A method for accurately predicting solvation structure. *J. Chem. Theory Comput.* **16**, 5401–5409 (2020).
- [24] Furness, J. W., Kaplan, A. D., Ning, J., Perdew, J. P. & Sun, J. Accurate and Numerically Efficient r2SCAN Meta-Generalized Gradient Approximation. *J. Phys. Chem. Lett.* **11**, 8208–8215 (2020).
- [25] Dasgupta, S., Lambros, E., Perdew, J. P. & Paesani, F. Elevating Density Functional Theory to Chemical Accuracy for Water Simulations through a Density-Corrected Many-Body Formalism. *Nature comm* **12**, 6359 (2021).
- [26] Palos, E., Caruso, A. & Paesani, F. Consistent Density Functional Theory-Based Description of Ion Hydration Through Density-Corrected Many-Body Representations. *ChemRxiv* 10.26434/chemrxiv-2023-vp6ns-v2 (2023).
- [27] Sim, E., Song, S., Vuckovic, S. & Burke, K. Improving Results by Improving Densities: Density-Corrected Density Functional Theory. *J. Am. Chem. Soc.* **144**, 6625–6639 (2022).

- [28] Song, S. *et al.* Extending density functional theory with near chemical accuracy beyond pure water. *Nature Communications* **14**, 799 (2023).
- [29] Belleflamme, F. & Hutter, J. Radicals in aqueous solution: Assessment of density-corrected SCAN functional. *Phys. Chem. Chem. Phys.* 10.1039.D3CP02517A (2023).
- [30] Mater, A. C. & Coote, M. L. Deep Learning in Chemistry. *J. Chem. Inf. Model.* **59**, 2545–2559 (2019).
- [31] Noé, F., Tkatchenko, A., Müller, K.-R. & Clementi, C. Machine Learning for Molecular Simulation. *Annu. Rev. Phys. Chem.* **71**, 361–390 (2020).
- [32] Behler, J. Four Generations of High-Dimensional Neural Network Potentials. *Chem. Rev.* **121**, 10037–10072 (2021).
- [33] White, A. D. Deep Learning for Molecules and Materials. *Living Journal of Computational Molecular Science* **3**, 1499 (2022).
- [34] Kocer, E., Ko, T. W. & Behler, J. Neural Network Potentials: A Concise Overview of Methods. *Annu. Rev. Phys. Chem.* **73**, 163–186 (2022).
- [35] Wen, T., Zhang, L., Wang, H., E, W. & Srolovitz, D. J. Deep potentials for materials science. *Materials Futures* **1**, 022601 (2022).
- [36] Kolluru, A. *et al.* Open Challenges in Developing Generalizable Large Scale Machine Learning Models for Catalyst Discovery. *arXiv* arXiv:2206.02005 (2022).
- [37] Tokita, A. M. & Behler, J. Tutorial: How to Train a Neural Network Potential. *arXiv* arXiv:2308.08859 (2023).
- [38] Satorras, V. G., Hoogeboom, E. & Welling, M. E(n) Equivariant Graph Neural Networks. *arXiv* arXiv:2102.09844 (2021).
- [39] Batzner, S. *et al.* E(3)-Equivariant Graph Neural Networks for Data-Efficient and Accurate Interatomic Potentials. *Nat. Commun.* **13**, 2453 (2022).
- [40] Batatia, I. *et al.* The Design Space of E(3)-Equivariant Atom-Centered Interatomic Potentials. *arXiv* arXiv:2205.06643 (2022).
- [41] Tholke, P. & Fabritiis, G. D. TorchMD-NET: Equivariant Transformers for Neural Network based Molecular Potentials. *arXiv* arXiv:2202.02541 (2022).
- [42] Liao, Y.-l. & Smidt, T. Equiformer: Equivariant Graph Attention Transformer for 3D Atomistic Graphs. *ArXiv* arXiv:2206.11990 (2022).

- [43] Yao, K., Herr, J. E., Toth, D. W., Mckintyre, R. & Parkhill, J. The TensorMol-0.1 model chemistry: A neural network augmented with long-range physics. *Chem. Sci.* **9**, 2261–2269 (2018).
- [44] Yue, S. *et al.* When do short-range atomistic machine-learning models fall short? *J. Chem. Phys.* **154**, 034111 (2021).
- [45] Gao, A. & Remsing, R. C. Self-Consistent Determination of Long-Range Electrostatics in Neural Network Potentials. *Nat. Commun.* **13**, 1572 (2021).
- [46] Jacobson, L. D. *et al.* Transferable Neural Network Potential Energy Surfaces for Closed-Shell Organic Molecules: Extension to Ions. *J. Chem. Theory Comput.* **18**, 2354–2366 (2022).
- [47] Husic, B. E. *et al.* Coarse graining molecular dynamics with graph neural networks. *J. Chem. Phys.* **153**, 194101 (2020).
- [48] Loose, T. D., Sahrman, P. G., Qu, T. S. & Voth, G. A. Coarse-Graining with Equivariant Neural Networks: A Path Towards Accurate and Data-Efficient Models. *arXiv* arxiv:2309.09290 (2023).
- [49] Majewski, M. *et al.* Machine learning coarse-grained potentials of protein thermodynamics. *Nat. Commun.* **14**, 5739 (2023).
- [50] Wilson, M. O. & Huang, D. M. Anisotropic molecular coarse-graining by force and torque matching with neural networks. *J. Chem. Phys.* **159**, 024110 (2023).
- [51] Smith, J. S., Isayev, O. & Roitberg, A. E. ANI-1: An extensible neural network potential with DFT accuracy at force field computational cost. *Chem. Sci.* **8**, 3192–3203 (2017).
- [52] Onat, B., Cubuk, E. D., Malone, B. D. & Kaxiras, E. Implanted neural network potentials: Application to Li-Si alloys. *Phys. Rev. B* **97**, 1–9 (2018).
- [53] Zhang, L., Wang, H., Car, R. & Weinan, E. Phase Diagram of a Deep Potential Water Model. *Phys. Rev. Lett.* **126**, 236001 (2021).
- [54] Shi, Y., Doyle, C. C. & Beck, T. L. Condensed Phase Water Molecular Multipole Moments from Deep Neural Network Models Trained on Ab Initio Simulation Data. *J. Phys. Chem. Lett.* **12**, 10310–10317 (2021).
- [55] Guo, Z. *et al.* Extending the limit of molecular dynamics with ab initio accuracy to 10 billion atoms. *arXiv* arXiv:2201.01446 (2022).
- [56] Zhang, C., Yue, S., Panagiotopoulos, A. Z., Klein, M. L. & Wu, X. Dissolving salt is not equivalent to applying a pressure on water. *Nat. Commun.* **13**, 822 (2022).

- [57] Zhang, J., Pagotto, J. & Duignan, T. T. Towards predictive design of electrolyte solutions by accelerating *ab initio* simulation with neural networks. *J. Mater. Chem. A* **10**, 19560–19571 (2022).
- [58] Malosso, C., Zhang, L., Car, R., Baroni, S. & Tisi, D. Viscosity in water from first-principles and deep-neural-network simulations. *npj Comput. Mater.* **8**, 139 (2022).
- [59] Shi, Y., Lam, S. T. & Beck, T. L. Quasichemical theory and quantum simulation based deep-learning potentials for modeling molten salt thermodynamics. *Chem. Sci.* **13**, 8265–8273 (2022).
- [60] Dajnowicz, S. *et al.* High-Dimensional Neural Network Potential for Liquid Electrolyte Simulations. *The Journal of Physical Chemistry B* **126**, 6271–6280 (2022).
- [61] Wang, F. & Cheng, J. Automated Workflow for Computation of Redox Potentials, Acidity Constants and Solvation Free Energies Accelerated by Machine Learning. *J. Chem. Phys.* **157**, 024103 (2022).
- [62] Zhang, C., Yue, S., Panagiotopoulos, A. Z., Klein, M. L. & Wu, X. Why Dissolving Salt in Water Decreases Its Dielectric Permittivity. *Phys. Rev. Lett.* **131**, 076801 (2023).
- [63] Avula, N. V. S., Klein, M. L. & Balasubramanian, S. Understanding the Anomalous Diffusion of Water in Aqueous Electrolytes Using Machine Learned Potentials. *arXiv* arXiv:2307.15576 (2023).
- [64] Jacobson, L., Stevenson, J., Ramezanghorbani, F., Dajnowicz, S. & Leswing, K. Leveraging Multitask Learning to Improve the Transferability of Machine Learned Force Fields. *ChemRxiv* 10.26434/chemrxiv-2023-8n737 (2023).
- [65] Guo, J. *et al.* AL4GAP: Active Learning Workflow for generating DFT-SCAN Accurate Machine-Learning Potentials for Combinatorial Molten Salt Mixtures. *ChemRxiv* 10.26434/chemrxiv-2023-wzv3q (2023).
- [66] Collins, K. D. Charge Density-Dependent Strength of Hydration and Biological Structure. *Biophys. J.* **72**, 65–76 (1997).
- [67] Kalcher, I. & Dzubiella, J. Structure-Thermodynamics Relation of Electrolyte Solutions. *J. Chem. Phys.* **130**, 134507 (2009).
- [68] VandeVondele, J. *et al.* Quickstep: Fast and accurate density functional calculations using a mixed gaussian and plane waves approach. *Comput. Phys. Commun.* **167**, 103–128 (2005).

- [69] Marcus, Y. Effect of ions on the structure of water: Structure making and breaking. *Chem. Rev.* **109**, 1346–1370 (2009).
- [70] Skinner, L. B. *et al.* Benchmark oxygen-oxygen pair-distribution function of ambient water from x-ray diffraction measurements with a wide Q-range. *J. Chem. Phys.* **138**, 074506 (2013).
- [71] Medders, G. R., Babin, V. & Paesani, F. Development of a “first-principles” water potential with flexible monomers. III. Liquid phase properties. *J. Chem. Theory Comput.* **10**, 2906–2910 (2014).
- [72] Wang, J. *et al.* Machine Learning of Coarse-Grained Molecular Dynamics Force Fields. *ACS Cent. Sci.* **5**, 755–767 (2019).
- [73] E, W., Lei, H., Xie, P. & Zhang, L. Machine learning-assisted multi-scale modeling. *J. Math. Phys.* **64**, 071101 (2023).
- [74] Tanaka, K. & Nomura, M. Measurements of tracer diffusion coefficients of lithium ions, chloride ions and water in aqueous lithium chloride solutions. *Journal of the Chemical Society, Faraday Transactions 1: Physical Chemistry in Condensed Phases* **83**, 1779 (1987).
- [75] Friedman, H. L. Lewis-Randall to McMillan-Mayer Conversion for the Thermodynamic Excess Functions of Solutions. Part II. Excess Energy and Volume. *J. Solution Chem.* **1**, 413–417 (1972).
- [76] Simonin, J.-P. Study of Experimental-to-McMillan-Mayer Conversion of Thermodynamic Excess Functions. *Journal of the Chemical Society, Faraday Transactions* **92**, 3519–3523 (1996).
- [77] Herr, J. E., Yao, K., McIntyre, R., Toth, D. W. & Parkhill, J. Metadynamics for training neural network model chemistries: A competitive assessment. *J. Chem. Phys.* **148**, 241710 (2018).
- [78] Kaufman, B. *et al.* COATI: Multi-modal contrastive pre-training for representing and traversing chemical space. *ChemRxiv* 10.26434/chemrxiv-2023-bdkgm (2023).
- [79] VandeVondele, J. & Hutter, J. Gaussian basis sets for accurate calculations on molecular systems in gas and condensed phases. *J. Chem. Phys.* **127**, 114105 (2007).
- [80] Goedecker, S., Teter, M. & Hutter, J. Separable dual-space Gaussian pseudopotentials. *Phys. Rev. B* **54**, 1703–1710 (1996).
- [81] Sun, J., Ruzsinszky, A. & Perdew, J. P. Strongly constrained and appropriately normed semilocal density functional. *Phys. Rev. Lett.* **115**, 036402 (2015).

- [82] Hutter, J. <https://github.com/juerghutter/GTH/> (2021).
- [83] Miceli, G., Hutter, J. & Pasquarello, A. Liquid water through density-functional molecular dynamics: Plane-wave vs atomic-orbital basis sets. *J. Chem. Theory Comput.* **12**, 3456–3462 (2016).
- [84] Yao, Y. & Kanai, Y. Free energy profile of NaCl in water: First-principles molecular dynamics with SCAN and  $\omega$ B97X-V exchange-correlation functionals. *J. Chem. Theory Comput.* **14**, 884–893 (2018).
- [85] Martyna, G. J., Klein, M. L. & Tuckerman, M. Nosé–Hoover chains: The canonical ensemble via continuous dynamics. *J. Chem. Phys.* **97**, 2635–2643 (1992).
- [86] Guidon, M., Hutter, J. & VandeVondele, J. Auxiliary Density Matrix Methods for Hartree-Fock Exchange Calculations. *J. Chem. Theory Comput.* **6**, 2348–2364 (2010).
- [87] Pagotto, J., Zhang, J. & Duignan, T. T. Predicting the properties of salt water using neural network potentials and continuum solvent theory. *ChemRxiv* 10.26434/chemrxiv-2022-jndlx (2022).
- [88] Hockney, R. W. *Computer Simulation Using Particles* (A. Hilger, 1988).
- [89] Plimpton, S. Fast parallel algorithms for short-range molecular dynamics. *J. Comput. Phys.* **117**, 1–19 (1995).
- [90] Spivak, M. *et al.* VMD as a Platform for Interactive Small Molecule Preparation and Visualization in Quantum and Classical Simulations. *J. Chem. Inf. Model.* **63**, 4664–4678 (2023).
- [91] Hess, B., Holm, C. & van der Vegt, N. Modeling Multibody Effects in Ionic Solutions with a Concentration Dependent Dielectric Permittivity. *Phys. Rev. Lett.* **96**, 147801 (2006).
- [92] Wolfram Research Inc. Mathematica. Wolfram Research, Inc. (2019).
- [93] Rasaiah, J. C. & Friedman, H. L. Integral equation methods in the computation of equilibrium properties of ionic solutions. *J. Chem. Phys.* **48**, 2742–2752 (1968).
- [94] Vrbka, L. *et al.* Ion-specific thermodynamics of multicomponent electrolytes: A hybrid HNC/MD approach. *J. Chem. Phys.* **131**, 154109 (2009).
- [95] Herrington, T. M., Pethybridge, A. D. & Roffey, M. G. Densities of Aqueous Lithium, Sodium, and Potassium Hydroxides from 25 to 75 °C at 1 atm. *J. Chem. Eng. Data* **31**, 31–34 (1986).

- [96] Sipos, P. M., Hefter, G. & May, P. M. Viscosities and densities of highly concentrated aqueous MOH solutions ( $M^+ = Na^+, K^+, Li^+, Cs^+, (CH_3)_4N^+$ ) at 25.0°C. *J. Chem. Eng. Data* **45**, 613–617 (2000).
- [97] Lide, D. R. (ed.) *CRC Handbook of Chemistry and Physics, Internet Version* (Taylor and Francis, Boca Raton, FL, 2007).
- [98] Pitzer, K. S. & Mayorga, G. Thermodynamics of Electrolytes. II. Activity and Osmotic Coefficients for Strong Electrolytes with One or Both Ions Univalent. *J. Phys. Chem.* **77**, 2300–2308 (1973).
- [99] Kusalik, P. G. & Patey, G. N. The thermodynamic properties of electrolyte solutions: Some formal results. *J. Chem. Phys.* **86**, 5110–5116 (1987).
- [100] Yeh, I.-C. System-Size Dependence of Diffusion Coefficients and Viscosities from Molecular Dynamics Simulations with Periodic Boundary Conditions. *J. Phys. Chem. B* **108**, 15873–15879 (2004).